



## Thermodynamic Analysis of Glass Formation in Fe-B System

M. Palumbo, G. Cacciamani\*, E. Bosco and M. Baricco  
Dip. Chimica IFM and INFM/INSTM – Università di Torino  
\* Dip. Chimica e Chimica Industriale – Università di Genova  
Corresponding author: M. Baricco, marcello.baricco@unito.it

(Received October 31, 2001)

**Abstract.** A thermodynamic optimisation of the Fe-B system has been carried out in order to model metastable phases. Amorphous and  $Fe_3B$  metastable phases have been considered in the assessment in order to describe, from a thermodynamic point of view, the well known glass forming ability of this system. An excess specific heat has been considered for the liquid alloys in order to take into account ordering processes on undercooling. The glass transition has been considered as a second order transition between undercooled liquid and amorphous phases. The effect of lattice stabilities on assessment has been discussed considering different descriptions for the free energy of undercooled pure liquid Fe. The calculated stable and metastable phase diagrams are in good agreement with experimental data, as well as invariant equilibria and thermodynamic properties. The results evidence the existence of an excess specific heat for glass forming Fe-B liquid alloys, which allows a reasonable description of thermodynamic functions for all phases in a wide temperature range.

© 2002 Published by Elsevier Science Ltd.

### Introduction

Amorphous alloys may be prepared with various techniques. The solidification at high quenching rates ( $\sim 10^6$  K s<sup>-1</sup>) of molten alloys may lead to the undercooling of liquid down to glass transition temperature ( $T_g$ ) and it has been widely used for industrial productions of thin ribbons of metallic glasses [93Lie]. More recently, amorphous alloys with suitable compositions may be prepared by conventional casting techniques, which entail significantly lower quenching rates ( $\sim 10$  K s<sup>-1</sup>) and give bulk metallic glasses [98Ino]. Solid state amorphisation reactions, obtained by ball milling or by cold rolling, have also been investigated for the synthesis of amorphous alloys [91Koc].

Together with experimental investigations, thermodynamic approaches to the prediction of glass formation in metallic systems have been developed. The glass forming range (GFR) can be simply obtained from thermodynamic arguments considering  $T_0$  curves, which describe the loci of temperature-composition where the Gibbs energy of liquid and crystal phases is equal [90Bar, 94Bor, 98Kim1]. For compositions where  $T_0 > T_g$ , a partitionless solidification is thermodynamically favoured and glass formation is not possible. On the contrary, neglecting the formation of intermetallic compounds for kinetic reasons, the composition range where  $T_0 < T_g$  gives the GFR for a particular system. Combining thermodynamic and kinetic approaches to glass formation, an estimate of the critical cooling rate for glass preparation is also possible [88Sau]. Amorphous phases are typically treated as deeply undercooled liquids and different models have been proposed for the thermodynamic description of glass transition. Starting from the so-called "Kauzmann paradox", glass transition temperature may be taken as an isoentropic temperature ( $T_k$ ), where the entropy of the undercooled liquid is equal to that of the corresponding mixture of crystal phases. Such approach has been used to estimate GFR in several binary [90Bat, 94Bor] and ternary systems [98Kim1, 98Kim2]. More recently, glass transition has been described as a second order transition, in terms of a constant factor due to the amorphisation stabilisation of liquid phase via glass transition [00Sha].

The Fe-B system shows a significant GFR for composition close to Fe-rich eutectic [84Ant]. It has often taken as a model system for the understanding of glass formation and crystallisation in metallic systems

[81Kös]. Several thermodynamic assessments have been reported for stable Fe-B system [81Cha, 84Kau, 88Oht, 89Pan, 94Hal]. The formation of amorphous and metastable crystal phases in Fe-B has been firstly considered in [83Shi]. The GFR in Fe-B has been estimated considering a constant specific heat for the liquid Fe in undercooling conditions [90Cla]. This approach gives an unsatisfactory description of the whole system [01Bos] because of the absence of excess specific heat contributions to the Gibbs free energy description of the undercooled liquid alloys. A more physical modelling of undercooled liquid phase in Fe-B has been recently reported [00Tol]. It is based on two level model [88Agr] and it has been used for the extrapolation of thermodynamic properties of undercooled Fe<sub>85</sub>B<sub>15</sub> liquid alloy.

The aim of this paper is to perform a reassessment of binary Fe-B phase diagram, considering the formation of amorphous and metastable crystalline phases. The role of the Gibbs free energy description of the undercooled liquid for pure elements and alloys is investigated in order to obtain a reasonable description of metastable phase diagram. From assessed thermodynamic functions, GFR is estimated.

### Phases Description

#### Pure elements

The SGTE description of lattice stabilities [91Din] ensures that the Gibbs energy curves of the liquid and solid phases intersect only at melting temperature (T<sub>m</sub>), avoiding the occurrence of an artificial phase stability and of the Kauzmann paradox [95Agr]. These conditions are obtained by a suitable description of the specific heat of undercooled liquid, so that its difference with the specific heat of stable crystal phases becomes zero at about 0.5 T<sub>m</sub>. This description of undercooled liquid is not based on physical arguments and it does not fully agree with experimental [84Per] and theoretical [95Mur] studies.

In present calculations, the lattice stabilities of solid phases have been taken according to SGTE extrapolation [91Din]. The Gibbs free energy of liquid Fe has been firstly taken from [91Din] and then according to [90Cla]. The Gibbs energy expression for metastable bcc and fcc pure B has been taken from [89Pan].

#### Solution phases

The excess Gibbs energy of the solution phases has been described in terms of Redlich-Kister polynomial:

$${}^{ex}G^\varphi = x_B x_{Fe} \sum_{v=0}^2 {}^vL^\varphi (x_B - x_{Fe})^v \quad (1)$$

where  ${}^vL^\varphi$  is the interaction parameter of the phase  $\varphi$ ,  $x_{Fe}$  and  $x_B$  are the molar fraction of Fe and B, respectively. A temperature dependence of interaction parameters has been considered only for the first term of the polynomial:

$${}^0L^\varphi = A_0^\varphi + B_0^\varphi \cdot T + C_0^\varphi \cdot T^{-1} \quad (2)$$

$C_0^l$  parameter is related to the presence of an excess specific heat in the undercooled liquid, which is proportional to  $T^{-2}$ , according to previous descriptions based on the hole theory of liquids [94Bor]. The excess specific heat contribution to the Gibbs free energy of the undercooled liquid disappears at glass transition, so that  $C_0^{am} = 0$  has been considered for amorphous phase. Glass transition has been considered as a second order transition, where  $\Delta S = \Delta H = \Delta G = 0$  between undercooled liquid and amorphous phases. The equalities of the free energies and entropies of liquid and amorphous phases at T<sub>g</sub> gives the following constraints between interaction parameters:

$$A_0^{am} = A_0^l + 2 \cdot C_0^l \cdot T_g^{-1} \quad (3)$$

$$B_0^{am} = B_0^l - C_0^l \cdot T_g^{-2} \quad (4)$$

Owing to the limited solubility of boron in bcc and fcc iron, solid solutions have been also described in terms of Redlich-Kister polynomial (eq.1) [94Hal]. The magnetic contributions to bcc solid solutions have been taken equal to those of pure Fe [91Din].

### Compounds

The Gibbs free energy of stable (FeB and Fe<sub>2</sub>B) and metastable (Fe<sub>3</sub>B) line compounds has been described according to:

$$\Delta G^{Fe_xB_y} = x^0 G_{Fe}^{\alpha} + y^0 G_B^{\beta} + \Delta H_{for} - T \cdot \Delta S_{for} \quad (5)$$

where  $\Delta H_{for}$  and  $\Delta S_{for}$  are the enthalpy and entropy of formation, respectively, and  $^0G_{Fe}^{\alpha}$  and  $^0G_B^{\beta}$  are the lattice stability of the standard reference state for Fe and B, respectively.

### Experimental data

The set of experimental data for stable equilibria have been taken from recent assessments [94Hal]. The metastable Fe<sub>3</sub>B compound has been reported as a crystallisation product of amorphous alloys in the composition range between 12 and 25 at % B [84Ant]. It decomposes to stable bcc-Fe and Fe<sub>2</sub>B after heating at high temperatures, as confirmed by recent calorimetric investigations [97Bat]. The enthalpy of formation of Fe<sub>3</sub>B has been estimated from the same experiments, where an eutectic temperature of 1387 K has been measured for metastable equilibrium between liquid and Fe<sub>3</sub>B + fcc-Fe. Fe<sub>3</sub>B has been reported with different structures [81Kos] but, owing to limited experimental data, a single phase has been considered in this work.

The glass transition temperature of amorphous Fe-B alloys is not available experimentally from DSC measurements. It has been observed at about 820 K for a Fe<sub>80</sub>B<sub>20</sub> amorphous alloy heated with an high speed calorimeter [83Hop]. Because T<sub>k</sub> corresponds to kinetic T<sub>g</sub> obtained at very low heating rate, a constant value of 800 K has been considered here for glass transition temperature. For the assessment of the Gibbs free energy of amorphous phase, the enthalpy of crystallisation of amorphous phase in the composition range between 12 and 25 at %B has been envisaged [84Ant]. In all cases, bcc Fe and Fe<sub>3</sub>B phases have been considered as crystallisation products.

Stable and metastable phase diagrams and thermodynamic functions have been assessed with ThermoCalc [93Jön].

## Results and discussion

### Equilibrium phase diagram

The equilibrium phase diagram has been assessed with  $C_0^l = 0$ , according to [94Hal]. The optimisation procedure started with liquid phase, considering partial molar enthalpy [75Esi] and activity [89Yuk] data. The partial molar enthalpies of mixing for B in liquid phase reported in [75Esi] have been neglected, because of an erroneous recalculation of reference states [94Hal]. The computed equilibrium phase diagram is shown in fig. 1 and the optimised values of model parameters are reported in Appendix (Stable). The relative standard deviation (RSD) for all parameters is rather low. A RSD value higher than 1 has been obtained only for B<sub>0</sub><sup>α</sup>, because of the lack of experimental data. The calculated invariant equilibria are reported in table I, together with corresponding experimental data. All types of reactions are calculated correctly. Temperatures and compositions of phases involved in invariant equilibria are reproduced within an error of less than 2%. Available data on melting temperature of FeB differ for more than 60 K [69Por, 77Sid] and the calculated value (1894 K) falls within uncertainty range. The invariant equilibrium between bcc, fcc and Fe<sub>2</sub>B is described as an eutectoid reaction, following experimental results [84Bro, 86Cam] and recent assessment [94Hal]. The comparison between calculated and experimental thermodynamic properties of intermetallic compounds is reported in table II. All calculated values have a satisfactory agreement with experimental data, except the enthalpy of fusion of FeB, which turns out higher with respect to the observed value.

### Metastable phase diagram

A metastable phase diagram has been calculated with  $C'_0 \neq 0$ , considering both amorphous and Fe<sub>3</sub>B as a new phase. So, experimental data related to these phases have been introduced in the optimisation procedure. In order to obtain a starting value for  $C'_0$  parameter, a similarity of the excess specific heat of undercooled liquid ( ${}^{ex}C'_p$ ) with specific heat difference between liquid and solid phases ( $\Delta C^{l-s}$ ) has been taken [87Bat]:

$$\Delta C^{l-s} \approx {}^{ex}C'_p = -2x_B x_{Fe} \cdot C'_0 \cdot T^{-2} \quad (6)$$

An average value of  $\overline{\Delta C^{l-s}}$  has been estimated for Fe<sub>83</sub>B<sub>17</sub> from calorimetric data [97Bat]. It turns out equal to 9 J mol<sup>-1</sup> K<sup>-1</sup> between T<sub>m</sub> and T<sub>g</sub> so that:

$$\overline{\Delta C^{l-s}} \approx {}^{ex}\overline{C'_p} = -\frac{x_{Fe} x_B C'_0}{T_m T_g} = 9 \text{ J mol}^{-1} \text{ K}^{-1} \quad (7)$$

For Fe<sub>83</sub>B<sub>17</sub> we have T<sub>m</sub>=1500 K and T<sub>g</sub>=800 K, which give -8·10<sup>7</sup> J mol<sup>-1</sup> K as a starting value for C'\_0.

Optimised values of the model parameters are reported in Appendix (Met1). All values show a RSD value significantly lower than 1. The equilibrium phase diagram, calculated according to new parameters, is reported in fig. 2. The metastable phase diagram has been calculated inserting Fe<sub>3</sub>B metastable intermetallic compound and suspending Fe<sub>2</sub>B phase. The results are also reported in fig. 2. Calculated invariant equilibria and thermodynamic properties are reported in table I and table II, respectively. All the results appear in good agreement with experimental data. The metastable eutectic reaction of the liquid into fcc and Fe<sub>3</sub>B is modelled in good agreement with experimental findings [97Bat]. A congruent melting of metastable Fe<sub>3</sub>B has been calculated at 1424 K, very close to a eutectic reaction of liquid with 25.7% at B which transform into Fe<sub>3</sub>B and FeB. Calculated and experimental values of the enthalpy of crystallisation of amorphous alloys are reported in fig. 3 as a function of composition. It appears clear that the presence on an excess specific heat in the undercooled liquid allows a better description of amorphous phase at low temperatures.

The temperature dependence of thermodynamic functions has been calculated for Fe<sub>83</sub>B<sub>17</sub>, which corresponds to the composition of stable Fe-rich eutectic. The enthalpy of undercooled liquid, amorphous and crystalline equilibrium phases is reported in fig. 4 as a function of temperature. The experimental data for enthalpies of crystallization ([84Ant]) and melting ([97Bat]) are also shown in fig. 4. The values of  $\Delta H_{cryst}$  and  $\Delta H_{melt}$  have been transformed into enthalpies of amorphous and liquid phases, respectively, by adding calculated enthalpies of corresponding solid phases. For Stable assessment, calculated enthalpy of liquid phase is significantly higher than experimental data. For Met1 assessment, the change in the slope of the curve for liquid phase at 800 K is associated to glass transition, whereas the step in the curve for solid mixture is due to the bcc-fcc allotropic transformation of iron. The agreement with calculated values is rather good both at high and low temperature, indicating a satisfactory description for thermodynamic properties of all phases in a wide temperature range.

The temperature dependence of the specific heat of liquid Fe<sub>83</sub>B<sub>17</sub> is shown in fig. 5. If the presence of an excess specific heat is not considered (Stable), it turns out simply as the weighted average of the specific heat of pure elements. According to the new modelling of liquid phase (Met1), liquid specific heat increases on undercooling and drops down at T<sub>g</sub> to the value of amorphous phase, close to that of solid mixture. A  $\Delta C_p$  value of about 20 J mol<sup>-1</sup> K<sup>-1</sup> is calculated at T<sub>g</sub>, in reasonable agreement with other glass forming systems [94Bor]. The specific heat of liquid Fe<sub>83</sub>B<sub>17</sub> reaches a minimum around eutectic temperature (1468 K) and shows a slope change at 1811 K. This behaviour is strongly related to the SGTE description for pure elements [91Din], so that the slope change of C<sub>p</sub> for pure Fe at T<sub>m</sub> is reflected even in liquid alloys. Moreover, the different modelling of undercooled liquid for pure elements and alloys produces the observed minimum of C<sub>p</sub>. In fact, according to the SGTE description of pure elements, the C<sub>p</sub> of the liquid is progressively reaching that of solid on undercooling. On the contrary, the effect of short range order in undercooled glass-forming alloys has been taken into account by the presence of an excess specific heat, described by C'\_0 parameter. As a consequence, the calculated excess

specific heat of liquid alloys must fully compensate the behaviour of pure elements and it may reach particularly high values. This effect is shown in fig. 6, where the  $C_p$  of liquid alloys at  $T_g$  (800 K) is reported as a function of composition. In absence of any experimental evidence of the composition dependence of excess specific heat, a parabolic trend has been taken from eq.1. It is worth noting that in order to have a reasonable description of thermodynamic properties of amorphous phase for compositions around the Fe-rich eutectic, a maximum value of more than 70 J mol<sup>-1</sup> K<sup>-1</sup> has been calculated for Fe<sub>50</sub>B<sub>50</sub> liquid alloy.

### Effect of lattice stabilities

In order to show the effect of lattice stabilities on the assessment of metastable phase diagrams, a constant value for the specific heat of undercooled Fe liquid ( $C_p^l = 46.0$ ) has been considered in the temperature range between  $T_m=1811$  K and  $T_g=800$  K ([90Cla]).

The values of new optimised parameters are reported in Appendix (Met2) and invariant equilibria and thermodynamic properties are reported in table I and II, respectively. Calculated values are again in reasonable agreement with experimental data. The presence of a specific heat for liquid Fe significantly higher than that of solid at  $T_g$ , strongly reduces the value of the  $^eC_p$  for liquid alloys, as shown in fig. 6. In addition, the calculated slope change of  $C_p^l$  in correspondence of the melting temperature of pure Fe is avoided, as shown in fig. 5. On the other hand, the calculated composition dependence of the heat of crystallisation of amorphous alloys, reported in fig. 3, does not fully fit the experimental data, because of an excessive stabilisation of undercooled liquid Fe. In conclusion, it appears evident that the description of pure components in undercooling conditions strongly influences calculated metastable phase diagrams.

### Calculation of the Glass Forming Range

The glass forming range in the Fe-rich side of Fe-B system has been calculated suspending all intermetallic compounds and considering  $T_0$  curves between liquid and solid solution phases. The value of  $T_0$  at  $T_g$  (800 K) represents the lower limit of glass forming range. The results are reported in fig.7a and 7b for fcc and bcc solid solutions, respectively. As concern GFR, the B-rich side is not considered in this work, because thermodynamic data related to amorphous phases are not available. In addition, Fe is considered insoluble in B, so that  $T_0$  curve cannot be calculated. The experimental limit of glass formation by rapid solidification, for low B content, is around 12% [84Ant], close to the value calculated by Stable assessment. As expected, the presence of an excess specific heat in undercooled liquid alloys (Met1), opens the glass forming range towards compositions with lower boron content. Rapid solidification of alloys with a B content lower than 9% gives Fe<sub>3</sub>B particles embedded in a bcc-Fe(B) solid solution ([87Bud]). The presence of a two phase mixture after rapid solidification, suggests a kinetic rather than a thermodynamic limit to glass formation for these compositions. So, wider GFR calculated with the contribution of an excess specific heat in Met1 represents a lower limit for thermodynamic constraints to glass formation. The stabilization of undercooled liquid pure Fe, introduced in the Met2 assessment, further extends calculated GFR to composition with a significantly lower boron content with respect to experimental data.

### Conclusions

Stable and metastable Fe-B phase diagrams have been assessed. An excess specific heat has been considered for liquid alloys in order to take into account ordering processes on undercooling. The specific heat of liquid alloys drops to a value close to that of solid mixture at glass transition. The metastable Fe<sub>3</sub>B has been also considered and its enthalpy and entropy of formation have been estimated. A constant value for the  $C_p$  of undercooled liquid Fe has also been considered for the assessment, but it leads to an excessive stabilization of the pure component. The results evidence the existence of an excess specific heat for glass forming Fe-B liquid alloys, which allows a reasonable description of thermodynamic functions for all phases in a wide temperature range.

### Acknowledgement

The authors like to remember fruitful collaboration with Himo Ansara. His suggestions and friendship will never be forgotten.

Work performed for CNR-PFMSTAII (97.00840.34) and RTN/BMG (HPRN-CT-2000-00033).

## References

- 69Por K. I. Portnoi, M. Kh. Levinshkaya, V. M. Romashov, *Sov. Powder Metall. Met. Ceram.* **8** (1969), 657.
- 70Vor L. G. Voroshin, L. S. Lyakhovich, G. G. Panich, G. F. Protasevich, *met. Sci. Heat Treat. (USSR)* **9** (1970), 732.
- 72Gor O. S. Gorelkin, A. S. Dubrovin, O. D. Kolesnikova, *Russ. J. Phys. Chem.* **46** (1972), 431.
- 72Plo A. F. Plotnikova, N. G. Ilyushchenko, A. I. Anfinogenov, C. I. Belyaeva, S. D. Finkelshteyn, *Tr. Inst. Electrochim. Ural Nauchn. Tsentr. Akad. Nauk. SSSR* **18** (1972), 112.
- 75Esi Yu. O. Esin, V. M. Baev, M. S. Petrushevskii, P. V. Gel'd, *Izv. Adak. Nauk. SSSR Met.* **4** (1975), 82.
- 77Sid F. A. Sidorenko, N. N. Serebrennikov, V. D. Budozhanov, Yu. V. Putintsev, S. N. Trushevskii, V. D. Korabanova, P. V. Gel'd, *High Temp.* **15** (1977), 36.
- 80Omo S. Omori, J. Moriyama *Trans. Jpn. Inst. Met.* **21** (1980), 790.
- 81Cha T. G. Chart, Comm. Comm. Eur. CECA No 7210-CA/3/303 (1981).
- 81Kös U. Köster, U. Herold, "Glassy Metals I" **46** (1981), 225.
- 82Sat S. Sato, O. J. Kleppa, *Metall. Trans. B* **13B** (1982), 251.
- 83Hop B. Hopstadius, G. Bäckström, *Internat. J. Thermophys.* **4** (1983), 235.
- 83Shi P. H. Shingu, "Amorphous Material – Physics and Technology", Ed. Committee of the Special Project Research on Amorphous Material (1983), 149.
- 84Ant C. Antonione, L. Battezzati, G. Cocco, F. Marino, *Z. Metallkde* **75** (1984), 714.
- 84Bro H. Brodosky, H. J. Wernicke, *CALPHAD* **8** (1984), 159.
- 84Kau L. Kaufman, B. Uhrenius, D. Birnie, K. Taylor, *CALPHAD* **8** (1984), 25.
- 84Per J. H. Perepezko, J. S. Paik, *J. of Non Crystalline Solids* **61** (1984), 113.
- 86Cam T. B. Cameron, J. E. Morral, *Metall. Trans. A* **17A** (1986), 1481.
- 87Bat L. Battezzati, A. L. Greer, *International J. of Rapid Solidification* **3** (1987), 23.
- 87But J. I. Budnick, F. H. Sanchez, Y. D. Zhang, M. Choi, W. A. Hines, Z. Y. Zhang, S. H. Ge and R. Hasegawa, *IEEE Transactions on Magnetics* **23** (1987), 1937.
- 88Ågr J. Ågren, *Phys. Chem. Liq.* **18** (1988), 123.
- 88Oht H. Ohtani, M. Hasebe, K. Ishida, T. Nishizawa, *Trans. Iron Steel Inst. Jpn.* **28** (1988), 1043.
- 88Sau N. Saunders, A. P. Miodownik, *Materials Science and Technology* **4** (1988), 768.
- 89Pan L. Pan, N. Saunders, presented at CALPHAD XVIII, Stockholm (1989).
- 89Yuk M. Yukinobu, O. Ogawa, S. Goto, *Metall. Trans. B* **20B** (1989), 705.
- 90Bar M. Baricco, L. Battezzati, *Key Engineering Materials* **48** (1990), 37.
- 90Bat L. Battezzati, M. Baricco, G. Riontino, I. Saletta, *Colloque de Physique C4* (1990), 79.
- 90Bor R. Bormann, R. Busch, *J. of Non Crystalline Solids* **117/118** (1990), 539.
- 90Cla M. T. Clavaguera-Mora, M. D. Baro, S. Suriñach, N. Clavaguera, *Colloque de physique C4* **14** (1990), 49.
- 91Din A. T. Dinsdale, *CALPHAD*, **15** (1991), 317.
- 91Koc C. C. Koch, "Materials Science and Technology" **15** (1991), 193.
- 93Jön B. Jönsson, B. Sundman, J. Ågren, *Thermochimica Acta* **214** (1993), 93.
- 93Lie H. H. Liebermann, "Rapidly Solidified Alloys", Marcel Dekker, Inc. New York (1993).
- 94Bor R. Bormann, *Materials Science and Engineering*, **A178** (1994), 55.
- 94Hal B. Hallemans, P. Wollants, J. R. Roos, *Z. Metallkde* **85** (1994), 676.
- 95Ågr J. Ågren et al., *CALPHAD* **19** (1995), 449.
- 95Mur B. S. Murty, M. M. Rao, S. Ranganathan, *CALPHAD* **19** (1995), 297.
- 97Bat L. Battezzati, C. Antonione, M. Baricco *J. of Alloys and Compounds* **247** (1997), 164.
- 98Ino A. Inoue, "Bulk Amorphous Alloys", Trans. Tech. Publications (1998).
- 98Kim1 Y. K. Kim, J. R. Soh, D. K. Kim, H. M. Lee, *J. of Non-Crystalline Solids* **242** (1998), 122.
- 98Kim2 Y. K. Kim, J. R. Soh, H. S. Kim, H. M. Lee, *CALPHAD* **22** (1998), 221.
- 00Sha G. Shao, *J. of Applied Physics* **88** (2000), 4443.
- 00Tol O. Tolochko, J. Ågren, *Journal of Phase Equilibria* **21** (2001), 19.
- 01Bos E. Bosco, M. Baricco, *La Metallurgia Italiana*, in press (2001).

## Appendix

Lattice stabilities			
	Stable	Met1	Met2
Fe liquid	from [91Din] (SGTE)	from [91Din] (SGTE)	from [90Cla]
Fe bcc, Fe fcc	from [91Din] (SGTE)	from [91Din] (SGTE)	from [91Din] (SGTE)
B liquid, B rhombohedral	from [91Din] (SGTE)	from [91Din] (SGTE)	from [91Din] (SGTE)
B fcc, B bcc	from [89Pan]	from [89Pan]	from [89Pan]

Phase	Parameters		
	Stable	Met1	Met2
liquid	${}^0L^{\text{liq}} = -106332 + 4.569 T$ ${}^1L^{\text{liq}} = 15844$ ${}^2L^{\text{liq}} = 46298$	${}^0L^{\text{liq}} = -47176 - 9.751 T - 5.929 \cdot 10^7 T^{-1}$ ${}^1L^{\text{liq}} = 15273$ ${}^2L^{\text{liq}} = 46567$	${}^0L^{\text{liq}} = -82770 - 0.428 T - 2.586 \cdot 10^7 T^{-1}$ ${}^1L^{\text{liq}} = 15549$ ${}^2L^{\text{liq}} = 47155$
amorphous	not present	${}^0L^{\text{am}} = -195390 + 82.884 T$ ${}^1L^{\text{am}} = 15273$ ${}^2L^{\text{am}} = 46567$	${}^0L^{\text{am}} = -65488 - 39.985 T$ ${}^1L^{\text{am}} = 15549$ ${}^2L^{\text{am}} = 47155$
Fe bcc ( $\alpha$ )	${}^0L^{\alpha} = -15878 + 1.768 T$	${}^0L^{\alpha} = -22131 + 7.036 T$	${}^0L^{\alpha} = -27512 + 11.983 T$
Fe fcc ( $\gamma$ )	${}^0L^{\gamma} = -49827 + 33.618 T$	${}^0L^{\gamma} = -57794 + 40.432 T$	${}^0L^{\gamma} = -68435 + 49.841 T$

$$G_{\text{ex}}^{\varphi} = x_B x_{\text{Fe}} \sum_{v=0}^2 {}^v L^{\varphi} (x_B - x_{\text{Fe}})^v$$

Redlich-Kister polynomials

Phase	Parameters		
	Stable	Met1	Met2
FeB	$\Delta H_{\text{for}} = -68000$ $\Delta S_{\text{for}} = -3.335$	$\Delta H_{\text{for}} = -68308$ $\Delta S_{\text{for}} = -3.963$	$\Delta H_{\text{for}} = -69120$ $\Delta S_{\text{for}} = -4.001$
Fe <sub>2</sub> B	$\Delta H_{\text{for}} = -81391$ $\Delta S_{\text{for}} = -3.204$	$\Delta H_{\text{for}} = -81226$ $\Delta S_{\text{for}} = -3.107$	$\Delta H_{\text{for}} = -79300$ $\Delta S_{\text{for}} = -1.914$
Fe <sub>3</sub> B	not present	$\Delta H_{\text{for}} = -76750$ $\Delta S_{\text{for}} = -2.596$	$\Delta H_{\text{for}} = -75895$ $\Delta S_{\text{for}} = -2.233$

$$\Delta G^{Fe_xB_y} = x {}^0G_{\text{Fe}}^{\alpha} + y {}^0G_{\text{B}}^{\beta} + \Delta H_{\text{for}} - T \cdot \Delta S_{\text{for}}$$

stoichiometric compounds Fe<sub>x</sub>B<sub>y</sub>

Table I Calculated and experimental invariant equilibria in the Fe-B system.

Reaction	Compositions of the respective phases (X <sub>B</sub> )			T (K)	Reference
liquid $\leftrightarrow$ FeB + $\beta$	.630	.500	1	1767	Stable
	.627	.500	1	1755	Met1
	.629	.500	1	1767	Met2
	.64	-	-	1773	[69Por]
liquid $\leftrightarrow$ FeB	0.500	0.500	-	1894	Stable
	0.500	0.500	-	1896	Met1
	0.500	0.500	-	1882	Met2
	-	-	-	1923	[69Por]
	-	-	-	1863	[77Sid]
liquid + FeB $\leftrightarrow$ Fe <sub>2</sub> B	0.335	0.500	0.333	1671	Stable
	0.343	0.500	0.333	1669	Met1
	0.337	0.500	0.333	1671	Met2
	0.33	-	-	1683	[69Por]
	0.325	-	-	1662	[70Vor]
$\delta \leftrightarrow \gamma +$ liquid	3.17 10 <sup>-4</sup>	1.11 10 <sup>-4</sup>	0.095	1662	Stable
	3.16 10 <sup>-4</sup>	1.09 10 <sup>-4</sup>	0.095	1662	Met1
	2.58 10 <sup>-4</sup>	7.57 10 <sup>-5</sup>	0.094	1662	Met2
	-	-	-	1654	[69Por]
liquid $\leftrightarrow$ $\gamma +$ Fe <sub>2</sub> B	0.168	2.07 10 <sup>-4</sup>	0.333	1468	Stable
	0.171	1.98 10 <sup>-4</sup>	0.333	1451	Met1
	0.169	1.57 10 <sup>-4</sup>	0.333	1452	Met2
	0.174	-	-	1473	[69Por]
	0.170	-	-	1447	[70Vor]
	0.170	-	-	1437	[97Bat]
$\gamma \leftrightarrow \alpha +$ Fe <sub>2</sub> B	5.91E-05	4.30 10 <sup>-5</sup>	0.333	1185	Stable
	5.91E-05	4.30 10 <sup>-5</sup>	0.333	1185	Met1
	5.91E-05	4.30 10 <sup>-5</sup>	0.333	1185	Met2
	5.90E-05	4.30 10 <sup>-5</sup>	-	1181	[86Cam]
liquid $\leftrightarrow$ $\gamma +$ Fe <sub>3</sub> B	0.186	2.19 10 <sup>-4</sup>	0.250	1386	Met1
	0.183	1.84 10 <sup>-4</sup>	0.250	1386	Met2
	-	-	-	1387	[97Bat]

Table II Calculated and experimental thermodynamic properties of intermetallic compounds in Fe-B system.

Compound	Property	Reference phases		T (K)	Calc. Stable (J/mol of atoms)	Calc. Met1 (J/mol of atoms)	Calc. Met2 (J/mol of atoms)	Experimental (J/mol of atoms)	Reference
		Fe	B						
Fe <sub>2</sub> B	Enthalpy of formation	α	β	298	-21000	-21000	-20300	-22300	[72Gor]
	Enthalpy of formation	γ	β	1385	-26400	-26300	-25700	-22600	[82Sat]
	Gibbs energy of formation	α	β	1173	-25600	-25600	-25400	-26000	[72Plo]
	Gibbs energy of formation	α	β	1100	-25600	-25600	-25400	-26400	[80Omo]
	Enthalpy of formation	α	β	298	-29400	-29600	-30000	-35600	[72Gor]
	Enthalpy of formation	γ	β	1385	-33450	-33600	-34000	-32300	[82Sat]
	Gibbs energy of formation	α	β	1173	-31800	-31600	-32000	-31800	[72Plo]
	Gibbs energy of formation	α	β	1100	-31900	-31700	-32100	-33300	[80Omo]
FeB	Enthalpy of fusion	-	-	1863	39400	38600	39100	31600	[77Sid]
	Entropy	-	-	298	19.7	19.4	19.4	18.1	[77Sid]
	Enthalpy of formation	γ	β	1385	-	-18300	-18100	-17840	[97Bat]
Fe <sub>3</sub> B	Enthalpy of formation	γ	β	1385	-	-	-	-	-

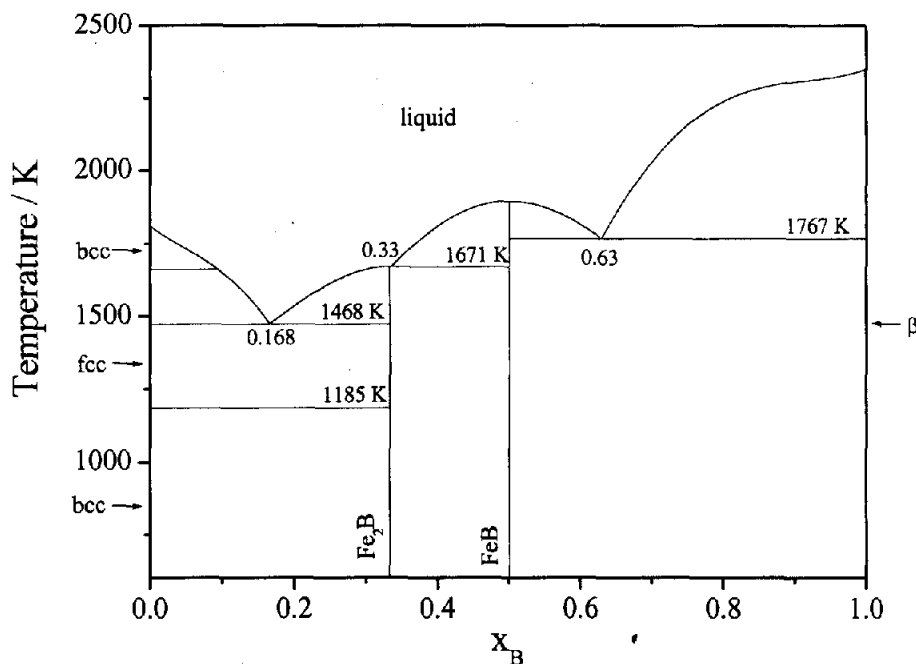


Fig. 1 Calculated Fe-B stable phase diagram (Stable)

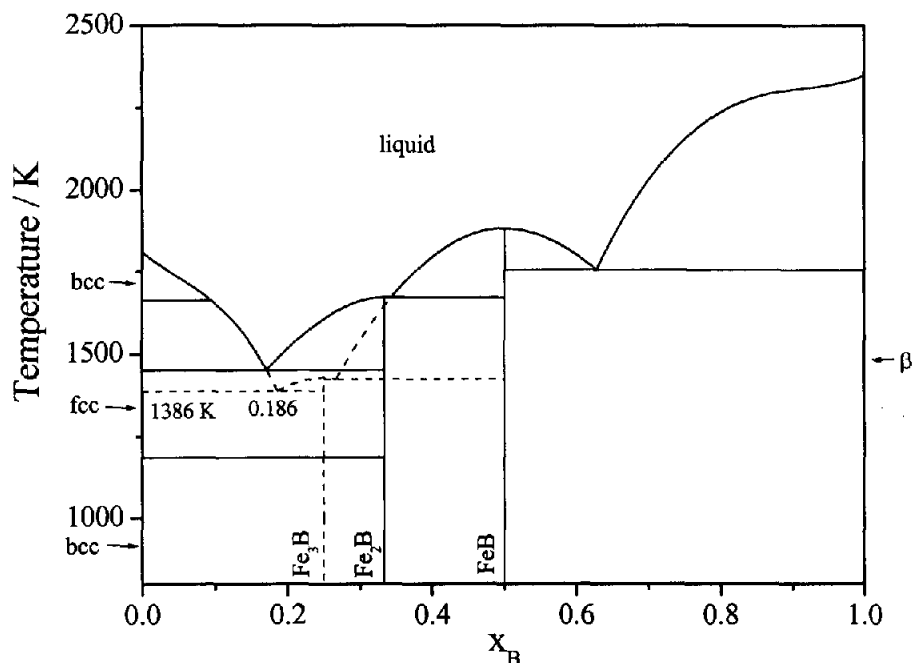


Fig. 2 Calculated Fe-B stable (continuous line) and metastable (dashed line) phase diagrams (Met1).

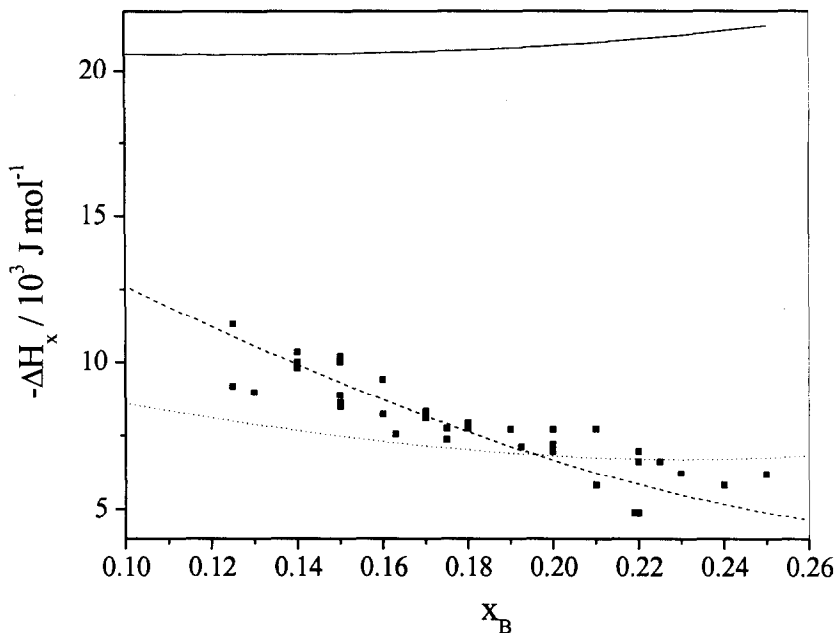


Fig. 3 Experimental and calculated enthalpy of crystallization of Fe-B amorphous alloys. Continuous line, Stable assessment; dashed line, Met1 assessment; dotted line, Met2 assessment; points, experimental data from [84Ant].

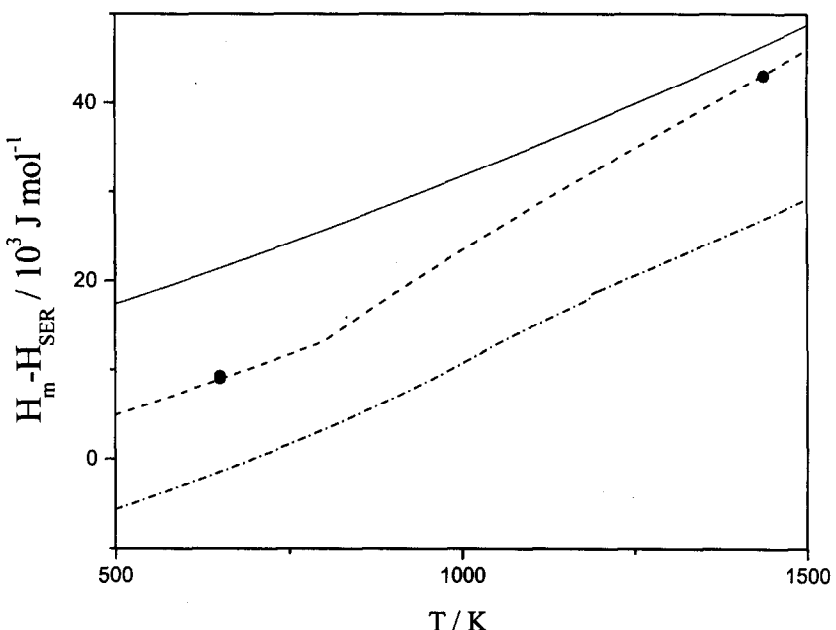
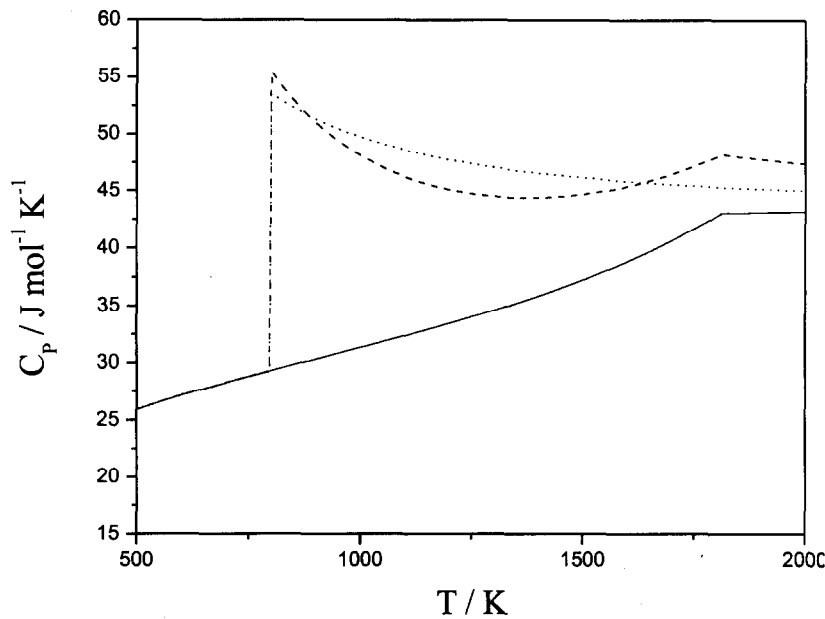
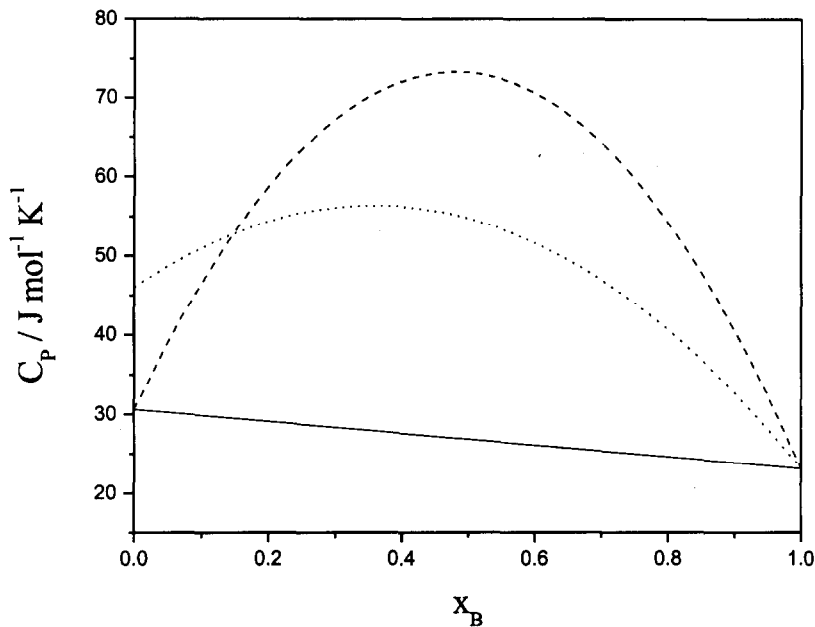


Fig. 4 Experimental and calculated enthalpy of liquid and solid phases for  $Fe_{83}B_{17}$  as a function of temperature. Continuous line, liquid phase (Stable); dashed line, liquid-amorphous phase (Met1); dashed dotted line, equilibrium solid mixture ( $Fe + Fe_2B$ ) (Met1).



**Fig. 5** Calculated specific heat of liquid phase for  $\text{Fe}_{83}\text{B}_{17}$  as a function of temperature. Continuous line, Stable assessment; dashed line, Met1 assessment; dotted line, Met2 assessment.



**Fig. 6** Calculated specific heat of undercooled liquid Fe-B alloys at 800 K as a function of composition. Continuous line, Stable assessment; dashed line, Met1 assessment; dotted line, Met2 assessment.

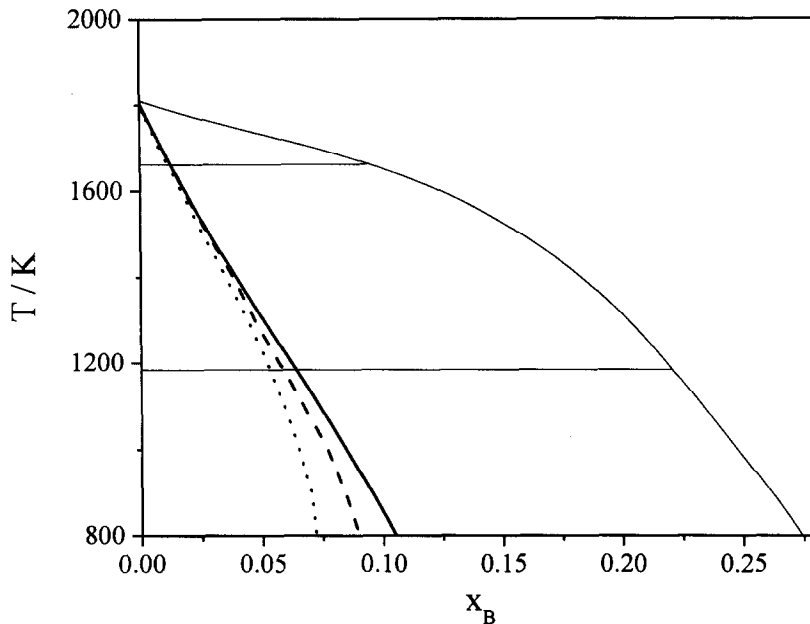


Fig. 7a  $T_0$  curves for fcc solid solution. Continuous line, Stable assessment; dashed line, Met1 assessment; dotted line, Met2 assessment.

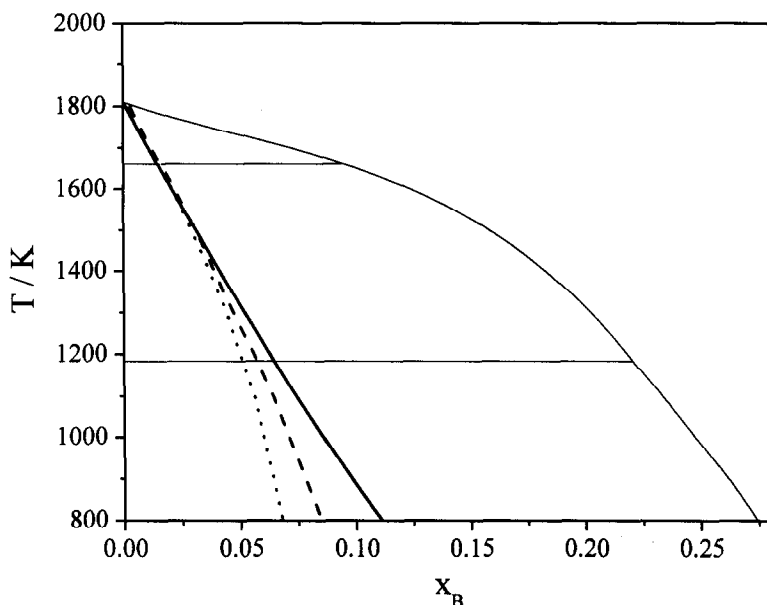


Fig. 7b  $T_0$  curves for bcc solid solution. Continuous line, Stable assessment; dashed line, Met1 assessment; dotted line, Met2 assessment.